Multiband Tight-Binding Model for Strained and Bilayer Graphene from DFT Calculations

T. B. Boykin[a], M. Luisier[b], N. Kharche[c], X. Jaing[c], S. K. Nayak[c], A. Martini[d], and G. Klimeck[e]
[a]ECE Department, The University of Alabama in Huntsville, Huntsville, AL 35899 USA
[b]Integrated Systems Laboratory, ETH Zurich, Gloriastrasse 35, 8092 Zurich, Switzerland
[c]Department of Physics, Applied Physics, and Astronomy, Rensselaer Polytechnic Institute, Troy, NY 12180 USA
[d]School of Engineering, University of California-Merced, Merced, CA 95343 USA
[e]Network for Computational Nanotechnology, School of ECE, Purdue University, West Lafayette, IN 47907 USA

***Abstract*—The single π–orbital model for graphene has been successful for extended, perfectly flat sheets. However, it cannot model hydrogen passivation, multi-layer structures, or rippled sheets. We address these shortcomings by adding a full complement of *d*-orbitals to the traditional {*s,p*} set. To model strain behavior and multi-layer structures we fit scaling exponents and introduce a long-range scaling modulation function. We apply the model to rippled graphene nanoribbons and bi-layer graphene sheets.**

Keywords-graphene, density-functional theory, tight-binding

I. INTRODUCTION

The single π–orbital Wallace model[1] has been successfully used to model extended, perfectly flat graphene sheets, where the bands decouple into two non-interacting sets, the σ– and π–bands; in this case the largely p_z-like π–bands are most relevant for transport. However, this model has significant limitations: artificial symmetries, and critically, no ability to model hydrogen-passivated nanoribbons (GNRs). Because experimental GNRs usually have passivated edges, the Wallace model[1] cannot simulate experiments. To remedy these problems we have recently developed a six-band {*p,d*} model for the π–bands of flat graphene[2].

Real graphene structures, in contrast, generally have ripples and corrugations: Ishigami, et. al.[3] find that graphene on $Si0_2$ substrates at least partially conforms to the substrate, with local strains up to 1%. These ripples couple the σ– and π–bands, so that a proper approach for device modeling such as graphene FETs[4], must reproduce both sets of bands, accommodate in- and out-of-plane strains, and accurately model the long-range interactions of bilayer graphene. Also, the approach must be computationally efficient and suitable for interfacing with other semiconductor tight-binding models in order to simulate devices with graphene active regions.

These requirements, together with the success of our six-band {*p,d*} model, point to an {*s,p,d*} model as the best compromise between accurate reproduction of the DFT graphene bands and computational efficiency. This approach has enough orbitals to permit fitting the graphene bands most involved in transport, as well as improving the ability to model the strain behavior of important gaps. The paper is organized as follows: Sec. II introduces the {*s,p,d*} model for both bulk and strained graphene and Sec. III presents the results of applying the model to rippled graphene nanostructures and bilayer graphene. Sec. IV presents our conclusions.

Identify applicable sponsor/s here. *(sponsors)*

II. MODEL

A. Bulk

In order to treat imperfect graphene sheets and nanostructures we have enlarged the customary graphene {*s,p*} model by adding all of the *d*-orbitals, similar to our expansion of the single π–orbital model[2]. For flat graphene the bands are decoupled as before: The σ–bands are spanned by $\{s,p_x,p_y,d_{xy},d_{x2\text{-}y2},d_{3z2\text{-}r2}\}$ and as before the π–bands by $\{ p_z,d_{yz}, d_{zx},\}$. Figure 1 shows the full graphene bands of our model along with the DFT+GW bands they are parameterized to fit. Lines show the tight-binding bands and symbols (diamonds) the DFT+GW bands. The bands reproduced by our model are also similar to those of a recent DFT calculation using *s*-, *p*-, and *d*-like localized basis functions[5].

The number and density of bands in the DFT+GW calculation show that no reasonably-sized tight-binding model will be able to reproduce the full bandstructure. Experience in attempting parameterizations of these bands, together with some characteristics of the {*s,p,d*} σ–bands, suggests that multiple *s*- and *p*-, and possibly multiple *d*-levels would be necessary to faithfully reproduce all of the bands in the energy range shown in Fig. 1. For example, the gap at Γ between the doubly-degenerate σ–valence- and conduction-bands remains mostly determined by the sum of *p*-orbital nearest-neighbor parameters $\left(V_{pp\sigma}+V_{pp\pi}\right)$. In spite of these limitations, the {*s,p,d*} basis for the σ–bands remains the best compromise between accuracy and efficiency. The computational cost of a multiple-{*s,p,d*} basis would exceed any potential benefit.

B. Strain

For small distortions (bond-length changes of a few percent), empirical tight-binding models customarily adopt a generalized Harrison-type (power-law) scaling:

$$V_{\alpha,\beta}(d) = \left(\frac{d}{d_0}\right)^{-\eta_{\alpha,\beta}} V_{\alpha,\beta}^{(0)} \tag{1}$$

where $V_{\alpha,\beta}(d)$ is a two-center integral, d is the actual bond-length, d_0 is the ideal bond-length, $V_{\alpha,\beta}^{(0)}$ is the ideal two-center integral, and $\eta_{\alpha\beta}$ the scaling exponent (positive). However, this behavior does not hold for large bond-length changes as exist in multi-layer graphene structures. Exponentials[7], powers modulated by a Fermi-Dirac cutoff[8] or products of powers and exponentials[9] have been employed as scaling functions to achieve faster decay at large bond-lengths. We have found an effective form to be a double-modulated scaling:

$$V_{\alpha,\beta}(d) = \left(\frac{d}{d_0}\right)^{-\eta_{\alpha,\beta}} V_{\alpha,\beta}^{(0)} f(d) \tag{3}$$

$$f(d) = \frac{1}{1+\exp\left[\alpha\left(d/d_0 - 1\right)\right]} + \frac{\left(d/d_0\right)^{\mu} \exp\left[\mu\left(1 - d/d_0\right)\right]}{1+\exp\left[-\alpha\left(d/d_0 - 1\right)\right]} \tag{4}$$

In Eqs. (3) and (4) we use the same Fermi cutoff parameter, α, and long-range scaling, μ, for all two-center integrals.

As shown in Figs. 2-3 this modulation function retains Harrison-type[6] scaling for small distortions while decaying more rapidly at longer ranges, as is necessary for modeling bi- and multi-layer graphene. The Harrison exponents[6] are fit to scaled DFT-gaps under hydrostatic and uniaxial [10] strain; the strain definition is given in Pereria, et. al.[7]. Although the basis set is expanded from the minimal tight-binding basis customarily employed, the number and density of DFT bands make it impossible to simultaneously fit all gaps under all strain conditions. We therefore concentrate on fitting the most important gaps for graphene nanostructures. Figs. 4 and 5 show the strain behavior of the two inequivalent M points under uniaxial [10] strain. A good fit is achieved for these gaps.

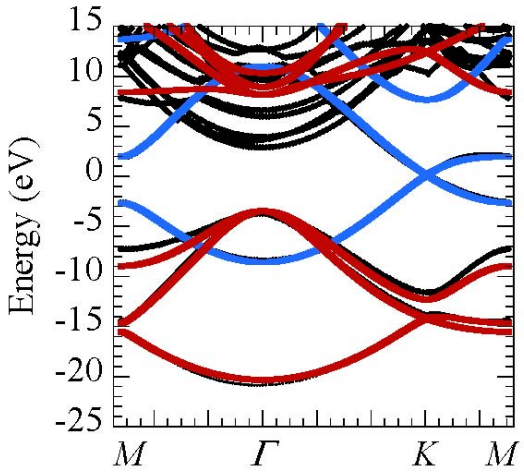

Figure 1: Bands of graphene as calculated with DFT+GW (solid black diamonds) and the tight-binding fit of the σ-bands (red lines) and π-bands (blue lines).

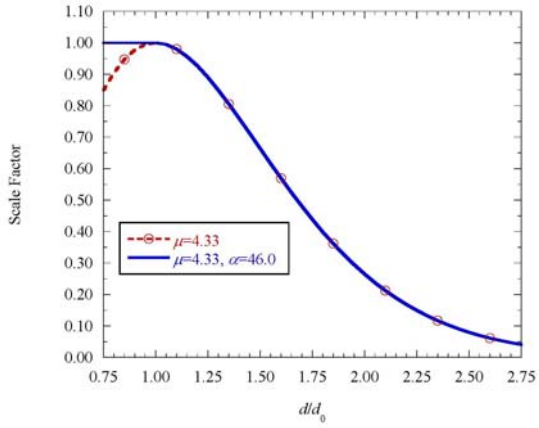

Figure 2: Full scaling function, eq. (4) (blue line), and numerator of second term of eq. (4), which controls the long-range behavior (red line with circles).

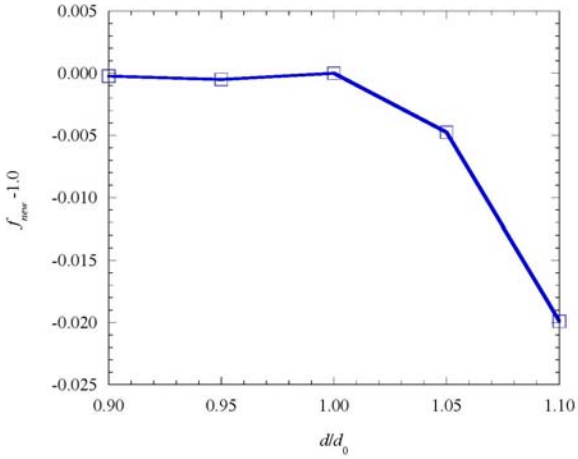

Figure 3: Deviation from 1.0 of full scaling function, eq. (4) (blue line with squares). Note that out to around +5% bond-length variation $f > 0.995$, thus preserving Harrison[6] scaling for small changes in bond-length.

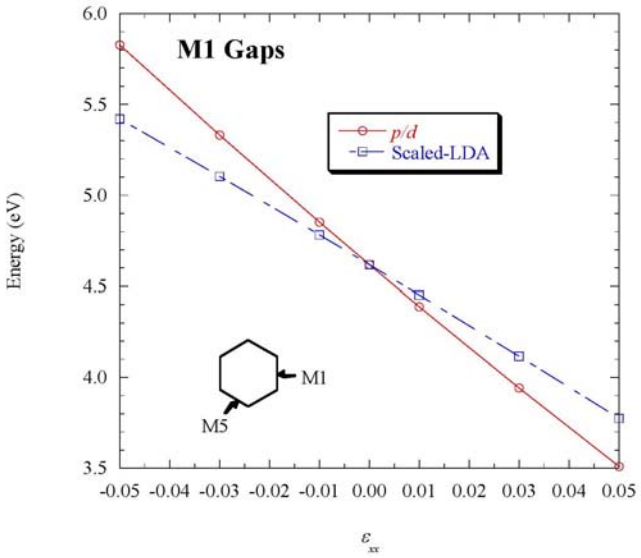

Figure 4: Behavior of the M1 gaps under uniaxial [10] strain. The DFT-LDA gap is scaled by the ratio of the zero-strain DFT+GW to DFT-LDA gap.

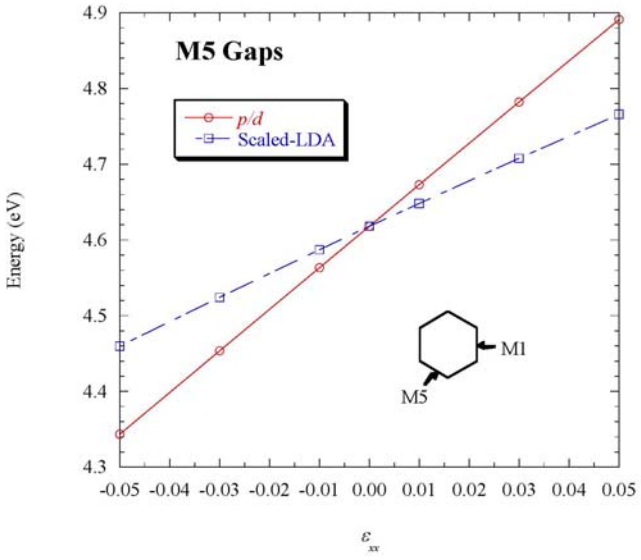

Figure 5: Behavior of the M5 gaps under uniaxial [10] strain. The DFT-LDA gap is scaled by the ratio of the zero-strain DFT+GW to DFT-LDA gap.

III. Results

We apply the model to rippled graphene nanostructures and bilayer graphene. The rippled armchair graphene nanoribbons are of with 8 nm and length 40, 70, or 100 nm; the ripples are determined with molecular dynamics simulations using LAMMPS[10]. For each length the transmission and resistance are the averages over 20 different samples; in the resistance calculation a small (0.1mV) bias is taken along the nanoribbon length.

Fig. 6 plots the averaged transmission through these nanoribbons as well as the transmission through an ideal nanoribbon ("ballistic"). Because the ripples are out-of-plane they induce couplings not only between bands in the respective σ– and π–sets but also between the σ– and π–bands. The transmission becomes very noisy with only vestiges of the stairstep behavior of the ballistic case. The resistance, Fig. 7, is seen to increase for longer nanoribbons due to increased scattering along the ribbon. Finally we calculate the tight-binding bands of bilayer graphene, as shown in Fig. 8. The bands exhibit the expected duplication along with a very small splitting at *K*.

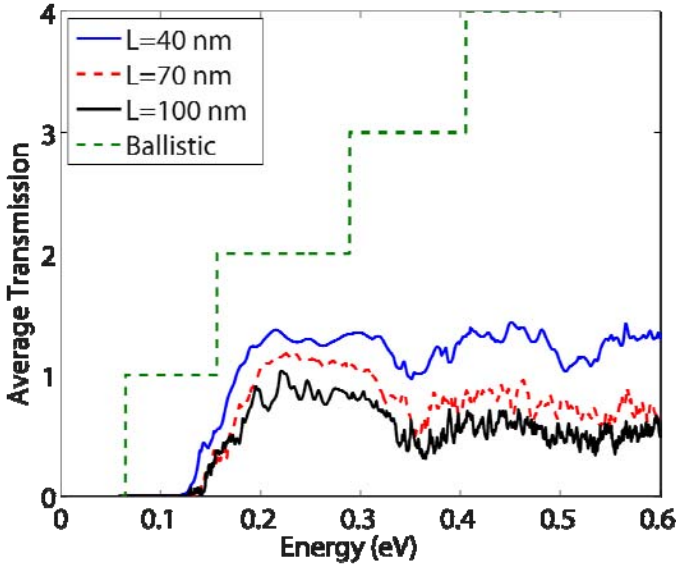

Figure 6: Transmission of 8 nm wide rippled graphene nanoribbons of various lengths. For reference, the transmission of a perfectly flat 8 nm nanoribbon is included ("ballistic").

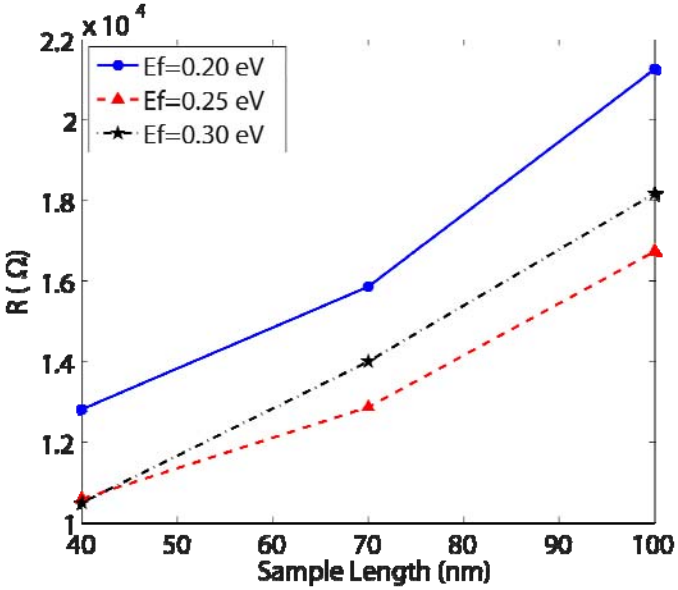

Figure 7: Resistance of 8 nm wide rippled graphene nanoribbons of differing lengths (40, 70, or 100 nm) at different Fermi levels. The zero of energy is taken at mid-gap (Γ) for each nanoribbon.

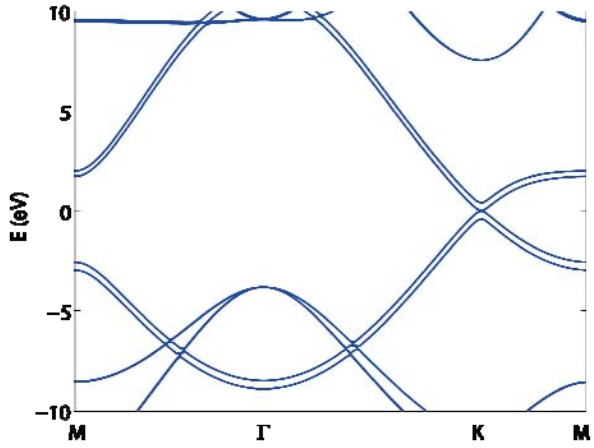

Figure 8: Bands of bilayer graphene as calculated with the {*s,p,d*} tight-biding model and our new scaling function, eq. (4).

IV. Conclusions

We have introduced an enhanced {*s*, *p*, *d*} model for graphene, in order to treat strained, rippled, and multi-layer structures. The bulk and strain parameters are optimized to reproduce DFT results for the technologically important gaps. Because Harrison-type[6] scaling does not work well for the long-range interactions of multi-layer graphene, we introduce a long-range scaling modulation function to treat these structures. We find that the model gives good results for rippled graphene nanoribbons as well as bi-layer graphene sheets.

Acknowledgment

This work was supported by NSF PetaApps grant no. OCI-0749140; NSF through XSEDE resources provided by the National Institute for Computational Science (NICS); MIND (NRI); and Interconnect Focus Centre (IFC).

References

[1] P. R. Wallace, "The Band Theory of Graphite," *Physical Review* **71**(9), pp.622-634, May 1947.

[2] T. B. Boykin, M. Luisier, G. Klimeck, X. Jiang, N. Kharche, Y. Zhou, and S. K. Nayak, *Journal of Applied Physics* **109**(10),104304, 15 May 2011

[3] M. Ishigami, J. H. Chen, W. G. Cullen, M. S. Fuhrer, and E. D. Williams, *Nano Letters* **7**(6), pp. 1643-1648, May 2011.

[4] G. Fiori and G. Iannaccone, "Simulation of Graphene Nanoribbon Field Effect Transistors," *IEEE Electron Device Letters* **28**(8), pp. 760-762, August 2007.

[5] R. M. Ribeiro and N. M. R. Peres, "Stability of boron nitride bilayers: Ground-state energy, interlayer distances, and tight-binding description," *Physical Review B* **83**(23), art. no. 235312, 15 June 2011.

[6] W. A. Harrison, *Elementary Electronic Structure*, (World Scientific, 1999).

[7] V. M. Pereria, A. H. Castro Neto, and N. M. R. Peres, "Tight-binding approach to uniaxial strain in graphene," *Physical Review B* **80**(4), art. no. 045401, 15 July 2009.

[8] J. L. Mercer and M. Y. Chou, "Tight-binding total energy models for silicon and germanium," *Physical Review B* **47**(15), pp. 9366-9376, 15 April 1993.

[9] L. Goodman, A. J. Skinner, and D. G. Pettifor, "Generating Transferable Tight-Binding Parameters: Application to Silicon," *Europhysics Letters* **9**(7), pp. 701-706, 1 August 1989.

[10] S. Plimpton, "Fast Parallel Algorithms for Short-Range Molecular Dynamics," *Journal of Computational Physics* **117**(1), pp. 1-19, 1 March 1995.